Electrochemically synthesised xanthone-cored conjugated polymers as materials for electrochromic windows

H.F. Higginbotham [a], M. Czichy [b], B.K. Sharma [c], A.M. Shaikh [c], R.M. Kamble [c], P. Data [a, b, d, *, 1]

[a] University of Durham, Physics Department, South Road, Durham, DH1 3LE, United Kingdom
[b] Faculty of Chemistry, Silesian University of Technology, M. Strzody 9, 44-100, Gliwice, Poland
[c] Department of Chemistry, University of Mumbai, Mumbai, 400 098, India
[d] Center of Polymer and Carbon Materials, Polish Academy of Sciences, M. Curie-Sklodowskiej 34, 41-819, Zabrze, Poland

ABSTRACT

In this work, we present the electrochemical polymerisation process of triarylamine-xanthone derivatives and behaviour of the formed polymers using various potentiodynamic techniques. The formed electropolymers have limited conjugation but show very promising electrochromic behaviour. Furthermore, by coupling the electrochemical analysis with each polymer's spectroscopic output, we were able to evaluate doping processes and the type of charge carriers formed. Through careful analysis, we were able to describe the electropolymerisation process and formed triarylamine-based polyxanthone derivatives. The polymers were found to exhibit good stability and good colouration efficiency to suggesting that they have potential application in electrochromic devices.

© 2018 The Author(s). Published by Elsevier Ltd. This is an open access article under the CC BY-NC-ND license (http://creativecommons.org/licenses/by-nc-nd/4.0/).

1. Introduction

All-organic electroactive materials have seen rapid growth in publication output and commercial development for use in optoelectronic applications [1,2] such as in organic light-emitting diodes (LEDs), photovoltaic cells, field-effect transistors [3,4] and lasers [5]. The current interest in these materials can be attributed to their surmounting practical benefits over heavy metal materials, including lower production cost, flexibility, and reduced environmental footprint.

For newly developed optoelectronic materials to be competitive with commercial counterparts they must contain properties that allow for the amelioration of device efficiency, lifetime and running or mass-production costs. This requires the production of new materials with good electrical conductivity, defined charge carrier balance and tuned transitional ground and excited states. Polymers

have been flagged as materials amenable to extend the potential of organic optoelectronics [6] due to the fact that they are easy to deposit [7,8] from spin-coated/solution processing techniques, creating layers that are less costly (when compared to vacuum deposition methods) and are known to form amorphous device layers [9,10] with fewer crystalline domains, resulting in improved reproducibility and transport characteristics [8]. Furthermore, polymeric materials display significant synthetic flexibility allowing for variable physical and electronic properties such as HOMO/LUMO band gaps [11] and emissive properties [6,12] as well as significant changes in carrier mobility and chemical stability [13,14].

Electropolymerisation has a long history [15], spanning back to the 1970s-1980s of polymerisation of aromatic heterocyclic materials such as anilines [16], fluorenes, thiophenes [17], carbazoles, pyrenes and indoles [18,19]. This technique has already been acknowledged as a unique method in order to create new electroactive materials with improved transport, thermal, and mechanical properties required for useful optoelectronic constituents [20], leading to cost-effective printing initiatives [21]. Electropolymerised conjugated compounds could also be used as unique materials for electrochromic windows in which electrochemical

---

doping causes changes in absorptivity due to the formation of polaronic/bipolaronic moieties in the polymer structure [22–26]. Such electrochromic windows could absorb in a broad range of the visible light spectrum [25–29], potentially creating black electrochromic materials [29–31].

Here we present an electrochemical investigation of three electroactive donor-acceptor-donor (D-A-D) materials, with triarylamines and xanthone to be used as electropolymerised materials for potential electroactive applications. While triarylamines such as diphenylamines (DPA) have already been shown to electropolymerise well [20,32–35], the mechanism of polymerisation, including polymerisation site, and extent of branching have been pinpointed using a combination of complimentary potentiodynamic techniques not previously highlighted in the literature. Furthermore, both DPA [36–39] and xanthones [40,41] have been shown to be useful electroactive materials for applications such as Organic Light Emitting Diodes (OLEDs) and so it was considered that merging these properties would obtain excellent materials for our investigation (Scheme 1) and has thus been proven to be useful materials for electrochromic windows, with comparable colour efficiency to the few literature examples [42–44].

2. Experimental section

2.1. Materials

All commercially available compounds were used as received. All solvents for the synthesis were dried and then distilled before use. Electrochemical measurements were performed in 10^{-3} M concentrations of the monomers. Electrochemical studies were conducted in 0.1 M argon purged solutions of Bu_4NBF_4 (dried), 99% (Sigma-Aldrich) in dichloromethane (DCM), CHROMASOLV®, 99.9% (Sigma-Aldrich) and acetonitrile, 99.9%, Extra Dry, AcroSeal™ (ACROS Organics) solvents at room temperature. UV–Vis–NIR spectroelectrochemical measurements were performed on an Indium Tin Oxide (ITO) coated quartz working electrode. Polymeric layers were synthesised on an ITO electrode in conditions similar to that of cyclic voltammetric measurements.

2.1.1. General synthesis

The detailed methodology for the synthesis of triarylamines based on xanthone is depicted in Scheme 2 and the molecular structures of the synthesised derivatives are illustrated in Scheme 1. The starting bromo derivative, 2,7–Dibromoxanthen–9–one required for the present study was synthesised according to the reported procedure [45] and the bromo precursor was conveniently converted to the triarylaminated derivatives by treating it with the corresponding diarylamine using a palladium catalysed Buchwald–Hartwig amination reaction [46,47], utilising palladium–bis(dibenzylideneacetone) [Pd(dba)$_2$] as a catalyst, 2–dicyclohexylphoshpino–2′,6′–dimethylbiphenyl (SPhos) as a ligand and sodium–tert–butoxide as a base, under nitrogen atmosphere for 12–24 h at 100 °C, giving derivatives **XDPAOMe**, **XNAP** and **XDPA** with a yield of more than 50% (**SI**) [48].

2.2. Measurements

^{1}H NMR spectra and ^{13}C NMR spectra were recorded using CDCl$_3$ on a Bruker 300 Ultrashield spectrometer with Tetramethylsilane (TMS) as an internal reference at a working frequency of 300 MHz and 75 MHz, respectively. Fourier transform infrared (FT-IR) spectra were recorded on a Perkin Elmer Frontier 91579. High Resolution Mass spectrometric measurements were recorded on a TOF Micromass YA−105 H < superscript></superscript> R−MS system. The electrochemical investigation was carried out using Autolab PGSTAT20 and PGSTAT100 (Metrohm Autolab) potentiostats. The electrochemical cell comprised of a platinum disk with 1 mm diameter of working area as the working electrode, silver wire electrode as the reference electrode and a platinum wire as the auxiliary electrode. The reference electrode was calibrated against a ferrocene/ferrocenium (Fc/Fc$^+$) redox couple in the same conditions (solvent, salt) for all electrochemical measurements. Cyclic voltammetry measurements were conducted at room temperature with a scan rate of 100 mV s^{-1}. UV−Vis−NIR spectra in the spectroelectrochemical analysis were recorded on a HP 8453 spectrometer and Ocean Optics QE6500. In situ EPR spectroelectrochemical experiments were performed using a JES-FA 200 (JEOL) spectrometer. The g-factor value was determined with the aid of a JEOL internal standard, knowing that the third line of the Mn-standard spectrum has a g-factor of 2.03324. The width of the EPR signal has been calculated as a distance in mT between the minimum and the maximum of the spectrum.

3. Results and discussion

3.1. Electrochemical investigation of monomers and electropolymerisation

Electrochemical and spectroelectrochemical studies of the three materials show remarkably different responses and their electropolymerisation (or lack thereof) was analysed using various electrochemically driven techniques. CV of **XDPAOMe** shows a 3-step oxidation with no discernible reduction step in dichloromethane solvent (Fig. 1a and supplementary Fig. S1a). Within the oxidation window, there are two reversible redox couples close to each other at +0.32 V and +0.45 V and a single irreversible oxidation peak at +0.90 V. During consecutive positive potential sweeps of **XDPAOMe**, no side reactions are observed. The good reversibility of the redox process could be explained due to its molecular structure. As **XDPAOMe** contains methoxy units in the 4 position of the DPA donor benzenes, these moieties block the oxidative active site and subsequently remove the possibility of side reactions occurring on the working electrode.

CV of **XNAP**, on the other hand, displays shows two reversible redox couples at +0.55 and + 0.70 V (Fig. 1b). As seen in **XDPAOMe**, no reduction of the xanthone moiety is observed (Supplementary Fig. S1c). Continual oxidative sweeps reveal the growth of an electropolymer, (**polyXNAP**), upon the working electrode, indicated by a sharp increase in peak current. The converging of oxidation peaks in subsequent scans to one value equal to +0.65 V
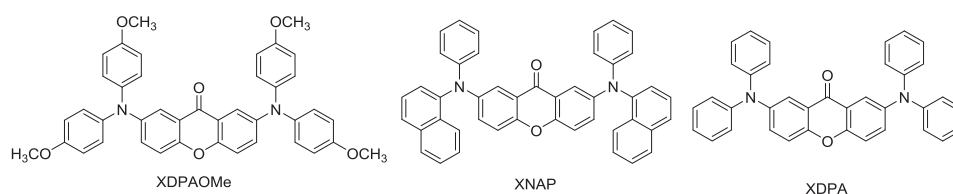
Scheme 1. Monomers studied in this work.
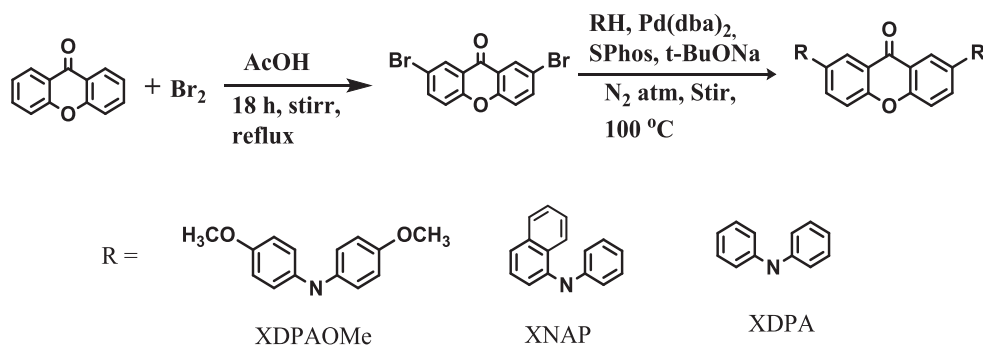
Scheme 2. Synthetic route used to obtain investigated monomers.
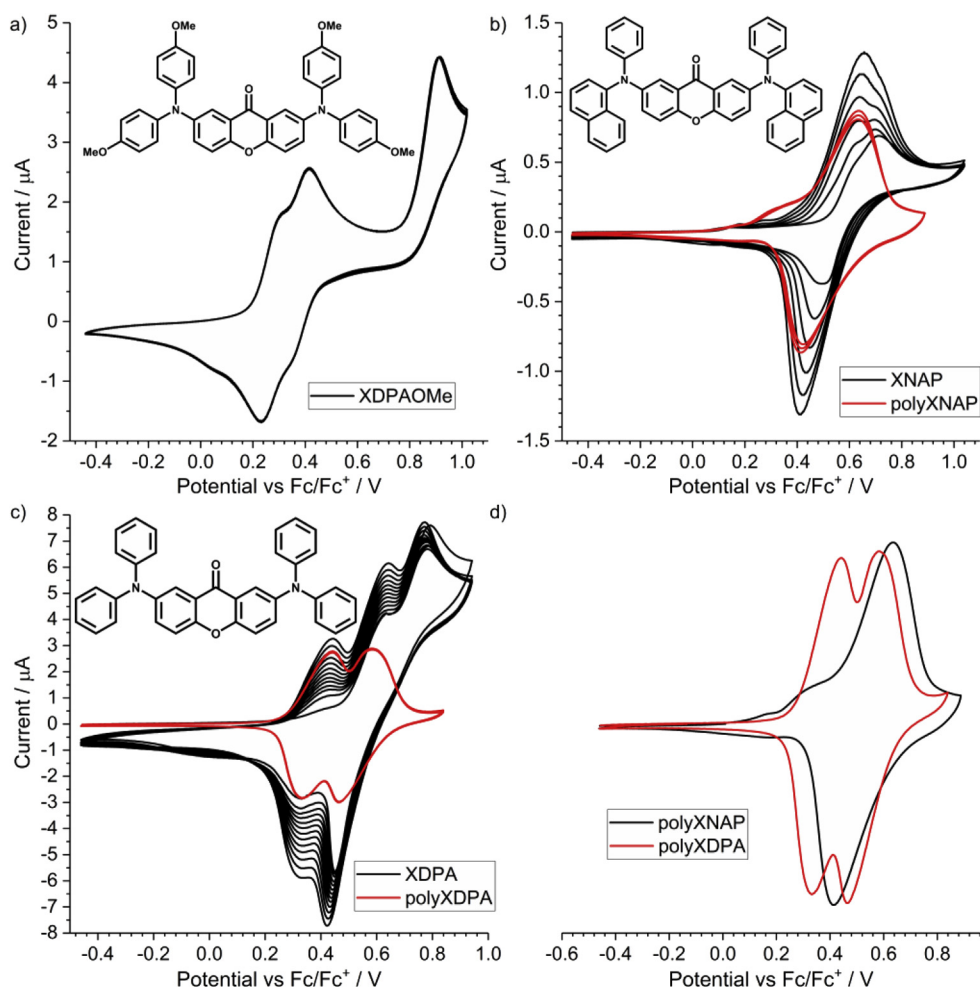
Fig. 1. a) Cyclic voltammograms of **XDPAOMe** showing oxidation/reduction cycles. Cyclic voltammograms showing the electropolymerisation process in consecutive scans (black line) of **XNAP** (b) and **XDPA** (c) monomers; Stability of the polymer recorded in monomer-free solution (red line). d) Comparison of cyclic voltammograms of synthesised polymers. CV recorded in DCM solutions of 0.1 M Bu$_4$NBF$_4$ supporting electrolyte. Scan rate 0.05 V s^{-1}. (For interpretation of the references to colour in this figure legend, the reader is referred to the Web version of this article.)

is proof of delocalisation of the radical in a double-charged system (Scheme 3).

In turn, a significant increase in peak current can indicate, that only one resonance structure is preferential for coupling, creating a synthetic link *via* only one phenyl group per one monomer unit, leaving an unchanged naphthalene in the lateral positions (Scheme 4). Moreover, **polyXNAP** appears to be highly stable as numerous potential sweep cycles between −0.5 and 0.9 V displays no change

in the peak potential position or the peak current output (Fig. 1b). It should be noted, that such unchanging character of the CV also confirms the lack of consequent processes changing the structure of the polymer, e.g. coupling with the participation of naphthalene radicals in a side group: **polyXNAP**-1b, **polyXNAP**-2b (Scheme 3).

CV of **XDPA** oxidation in the first scan shows two well-separated reversible oxidative peaks at +0.60 V and +0.75 V (Fig. 1c), having similar behaviour as during **XDPAOMe** oxidation (Fig. 1a), which
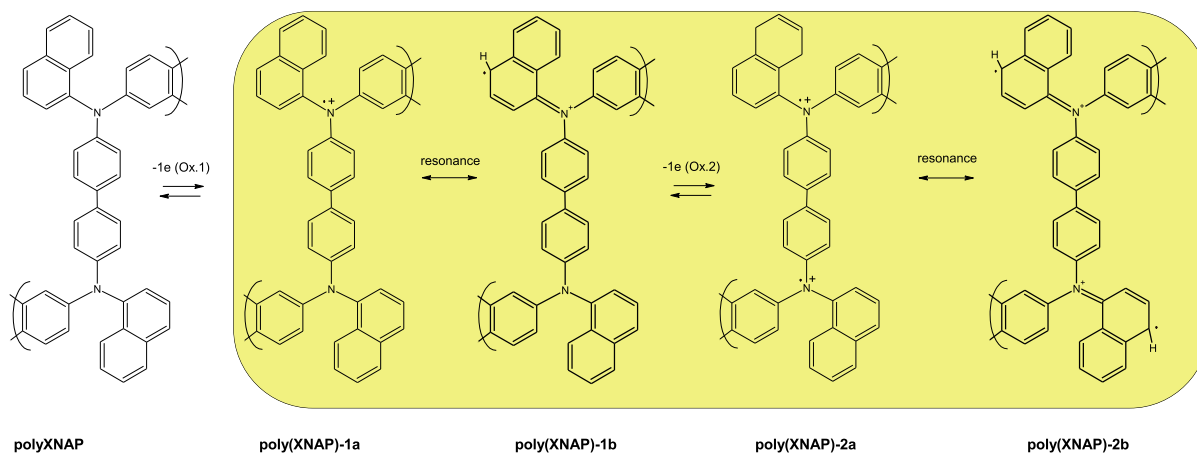
Scheme 3. Two-stage oxidation mechanism of **polyXNAP** with dominant resonance structures on a yellow background.
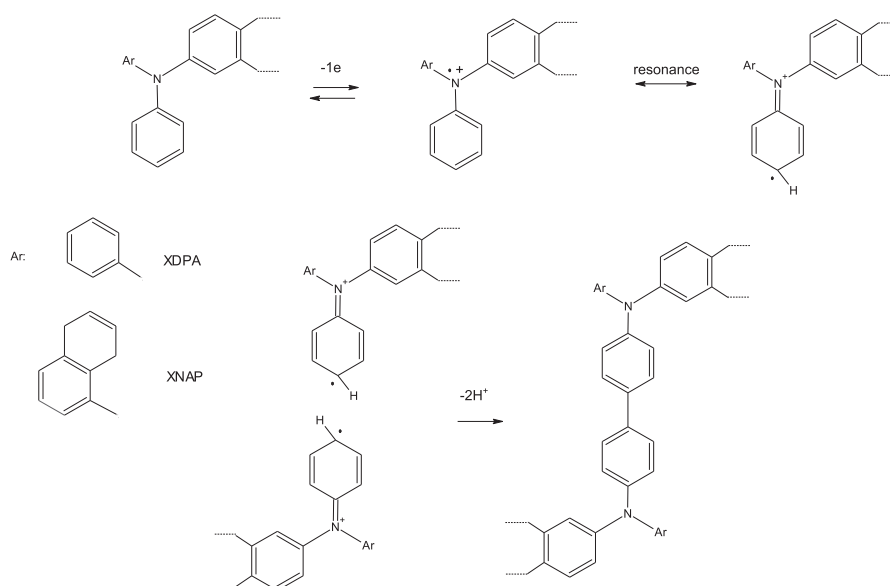
Scheme 4. Proposed mechanism of **XNAP** and **XDPA** electropolymerisation.

come from the radical cation and diradical dication, respectively. However, the peak potentials for the latter are considerably reduced, due to the presence of additional electron-donor groups in the phenyl rings. Without the presence of the 4-methoxy groups present in **XDPAOMe**, the proceeding CV cycles of **XDPA** see an additional peak at +0.35 V (Fig. 1c), confirming the oxidation of uncoupled phenyl groups (marked red, Scheme 5), which can be coupled to polymeric branched structures **polyXDPA** (Scheme 6). This is in contrast to **polyXNAP**, which shows a broad oxidative redox couple, linked to the formation of a delocalised diradical dication.

CV of **polyXDPA** oxidation shows two well-separated reversible oxidative peaks (Fig. 1d). We assigned the first wave (+0.60 V) to the oxidation of one of two triarylamine cores, resulting in the radical cation localised at the central part of the star-shaped skeleton **polyXDPA**-1a (Scheme 6). Further oxidation (+0.75 V) occurs at the second triarylamine units, **polyXDPA**-2a (Scheme 6).

Surprisingly, the **XDPAOMe** molecule had the lower electrochemical band-gap and oxidation potential compared to **XDPA** which probably is caused by a decrease of the phenyl ring rotation by the methoxy side group. This increases the conjugation length of

the molecule, creating stronger communication between the DPA and xanthone core (Table 1). Opposite behaviour was observed when phenyl and naphthyl group are compared, with the **XNAP** band-gap value slightly larger, which suggests slightly lower conjugation between the DPA and xanthone units (Table 1).

3.2. UV−vis spectroelectrochemical analysis of the investigated compounds

Spectroelectrochemical analysis of the **XDPAOMe** monomer reveals that while the neutral species of the monomer mirrors the steady-state absorption in solution (Supplementary Fig. S2), the formulation of new strongly vibronic bands with a peak maxima of ~371, 606 and 750 nm is observed upon application of positive potential, with and a maximum absorptivity at +0.48 V (Fig. 2a). The creation of these peaks have already been shown in literature in similar compounds containing DPA and is attributed to the formation of a radical cation upon each triarylamine moiety of **XDPAOMe** [35]. This cationic species is fully reversible with decreasing potential back down to 0 V (Supplementary Fig. S1b). UV−vis spectroelectrochemistry of **polyXNAP** oxidation at +0.5 V
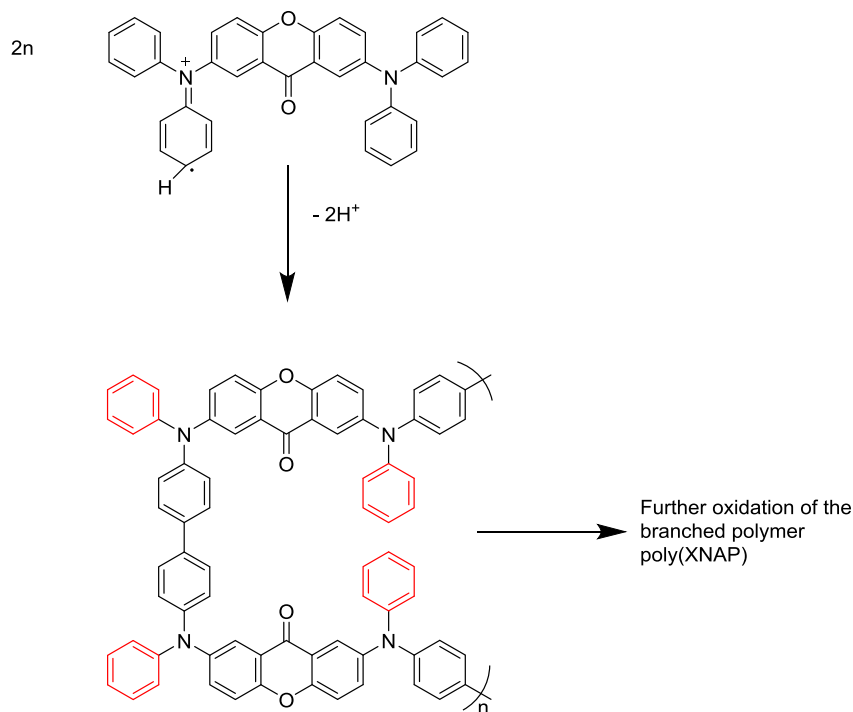
Scheme 5. Phenyl substituents in **polyXDPA** oxidizing at the +0.35 V.
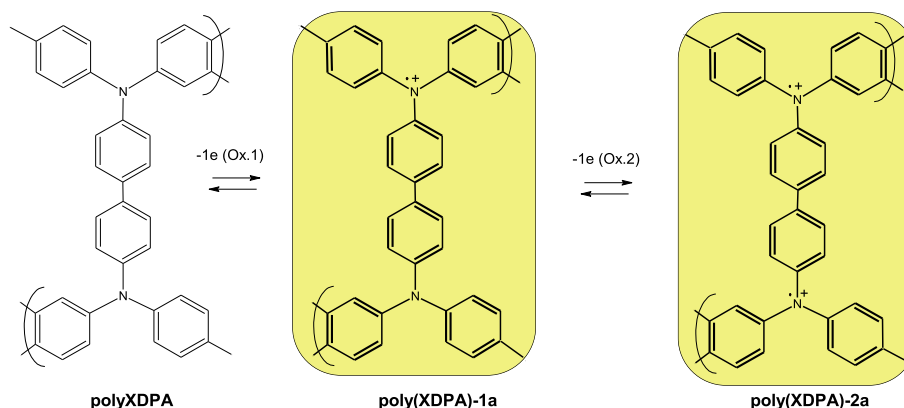
Scheme 6. Two-stage oxidation mechanism of **polyXDPA**, with one resonance structure (yellow background) at each stage.

Table 1
Electrochemical and spectroscopic properties of investigated molecules.

Compound/polymer	E_{ox}^{onset}, V[a]	E_{red}^{onset}, V[b]	IP, eV[c]	EA, eV[d]	E_g^{el}, eV[e]
XDPAOMe	0.20	−2.01	−5.3	−3.09	2.21
XNAP	0.52	−2.08	−5.62	−3.02	2.6
XDPA	0.50	−2.05	−5.6	−3.05	2.55
polyXNAP	0.41/0.19	−1.99	−5.51	−3.11	2.4
polyXDPA	0.26	−1.97	−5.36	−3.13	2.23

[a] *Onset* oxidation potential.
[b] *Onset* reduction potential.
[c] Ionization potential IP $= |e| (E_{ox}^{onset}+5.1)$.
[d] [49–51] Electron affinity EA $= |e| (E_{red}^{onset}+5.1)$ [49–51].
[e] Electrochemical energy gap $E_g^{el} = |e| (E_{ox}^{onset} - E_{red}^{onset})$ [49–51]; Electrochemical potentials given are relative to ferrocene/ferrecinium (Fc/Fc$^+$) redox couple.

shows the formation of a single broad band at λ_{max}~790 nm, thus coming from the diradical dication, whose electrons are strongly delocalised, (Fig. 2b).

UV−vis spectroelectrochemical analysis of **polyXDPA** shows the growth of a cation radical at an absorption maximum of 500 nm and one at over 1000 nm, with the absorbance maximising at +0.41 V (Fig. 2c), which confirms the information obtained from CV analysis. As the potential is further increased these positively charged species reduced as a new band grows in at λ_{max}~700 nm peaking at +0.64 V, suggesting further oxidation to a diradical dication, whose spectral shape is identical to the band registered for the diradical dication of **XDPAOMe**.

3.3. EPR spectroelectrochemical analysis of the investigated compounds

EPR spectroelectrochemistry is a very useful tool to obtain information about the position of unpaired electrons on the molecule's structure. In the case of **XDPAOMe**, the location of the dication can be pinpointed to the nitrogen atom using electrochemical-EPR analysis (g = 2.0026) [52]. At a potential
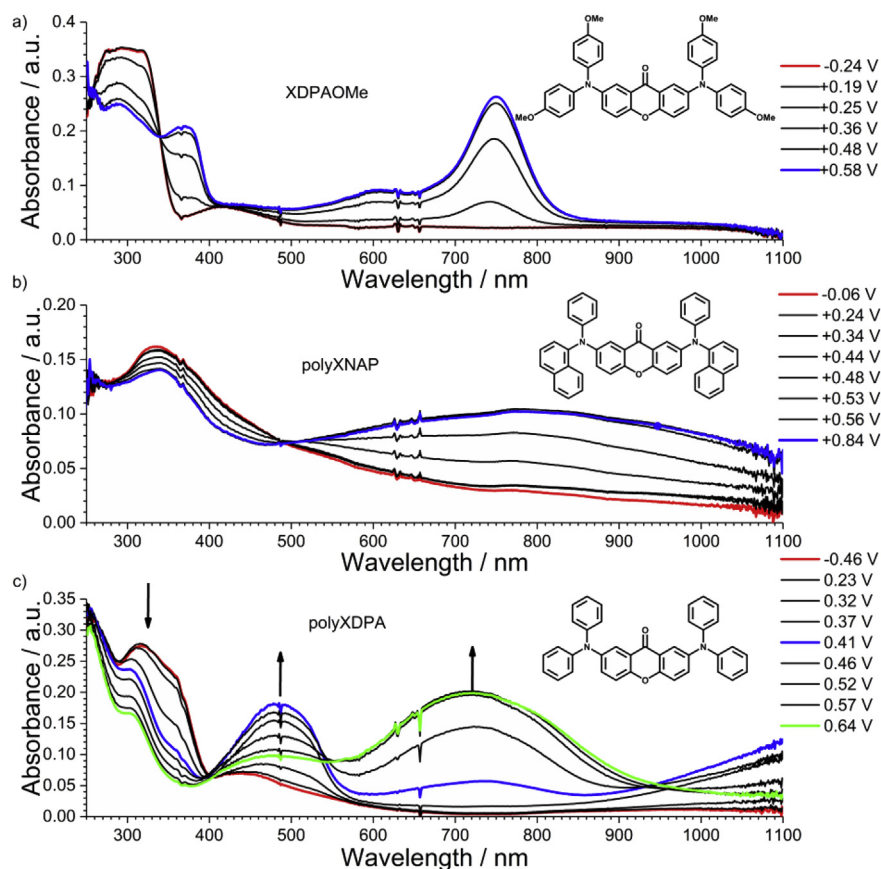
Fig. 2. UV–vis spectroelectrochemistry of **XDPAOMe** (a), **polyXNAP** (b) and **polyXDPA** (c) in 0.1 M Bu$_4$NBF$_4$ electrolyte in acetonitrile at potentiostatic conditions.

of +0.53 V, a clear absorption signal is displayed with paramagnetic triplet character (Fig. 3a), isolated on the nitrogen atoms, in which hyperfine coupling highlights that the unpaired electrons of the nitrogen nuclei interact with the protons of the phenyl group and the xanthene. The generation of this diradical dication is also fully reversible, as sweeping the potential back down to 0 V recreates the pair-spin neutral species which is again silent in regards to EPR. As for **polyXNAP**, EPR results confirm strong delocalisation of the diradical dication moiety on the molecular structure where the signal of the radical cation of **polyXNAP** was recorded at +0.54 V (Fig. 3b). The low g-factor of 2.0023 indicates greater electron delocalisation than in the case of ionised **XDPAoMe**, therefore, it is evident that alkoxy peripheral substituents can influence the reorganization energies and the electron delocalisation of these molecules [53]. Both the UV–vis spectroelectrochemistry and the EPR of **polyXNAP** were found to be fully reversible as in the former technique sweeping the potential back down to 0 V returns the spectra to its original high energy π-π* transitions below 450 nm (Supplementary Fig. S1d), while within the latter technique sweeping the potential back down to 0 V, recreates the silent pair-spin neutral species.

EPR of **polyXDPA** shows that a signal at a potential of +0.39 V, observed as a multitude of overlying signals, due to the hyperfine coupling of the unpaired electron to multiple nuclear spins (2.0022) (Fig. 3c). Upon increasing the potential to +0.74 V the signal widens from 0.17 mT to 0.19 mT and is shifted to a higher value of g = 2.0024, confirming that the unpaired electrons of the diradical dication display stronger hyperfine coupling to the nitrogen atoms, creating a stable polymeric molecule.

3.4. Electrochromic windows

As a final step and using the conclusions drawn from the spectroelectrochemical analysis, electrochromic windows were formed from the two electrochemically synthesised polymers. Polymers were synthesised in the same conditions presented in Fig. 1 but 50 scans were completed to obtain a thick film on an ITO electrode. Transmittance analysis of potentiostatic switching between potentials −1.0 V–1.0 V (Fig. 4) allowed for the characterisation of the intensity of colour change during electrochemical doping (contrast ratio CR), λ$_{max}$ of the doped form, colouration efficiency (CE) and optical density (ΔOD) (Table 2).

The electrochemical and spectroelectrochemical analysis shows that the **XNAP** compound forms a lower conjugated polymeric derivative due to the naphthalene steric hindrance. Although the formed polymers are conductive, the stability is much lower in **polyXNAP** when compared to the **polyXDPA** response. Similar behaviours are observed in the electrochromic analysis. The intensity of change of **polyXNAP** decreased with every working cycle to 73% after 100 cycles. **PolyXPDA** showed the much better stability of the doping-dedoping process where after 100 cycles the intensity of change decreased to only 87% of its 1st cycle (Fig. 4). The optical response time is slightly better for **polyXNAP**, however, due to its high optical density and low charge density the better polymer for future applications would be **polyXDPA** derivatives, showing almost 300 cm^2/C colouration efficiency (Table 2) and high contrast ratio which is very important for application purpose, where the amount of passed light must be significantly filtered.
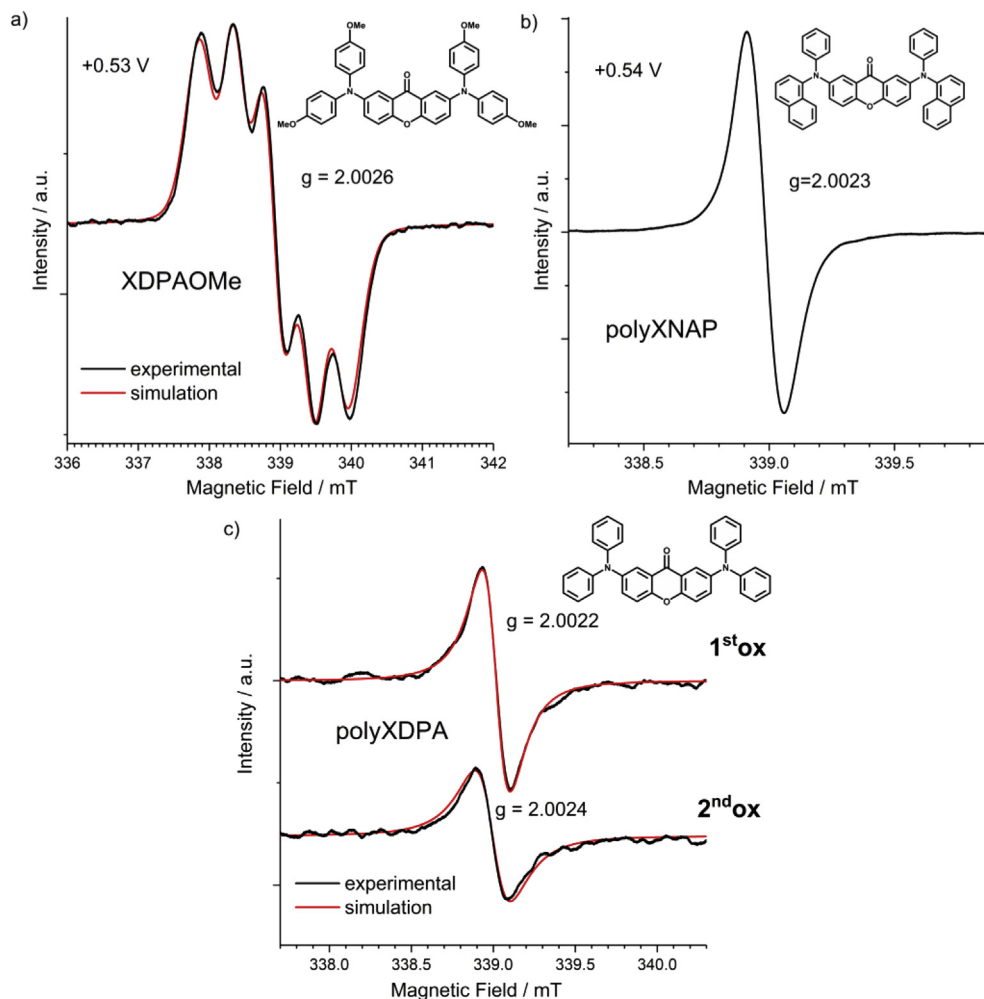
Fig. 3. EPR spectrum of 1 mM **XDPAOMe** (a), **polyXNAP** (b) and **polyXDPA** (c) in 0.1 M Bu$_4$NBF$_4$ electrolyte in DCM.
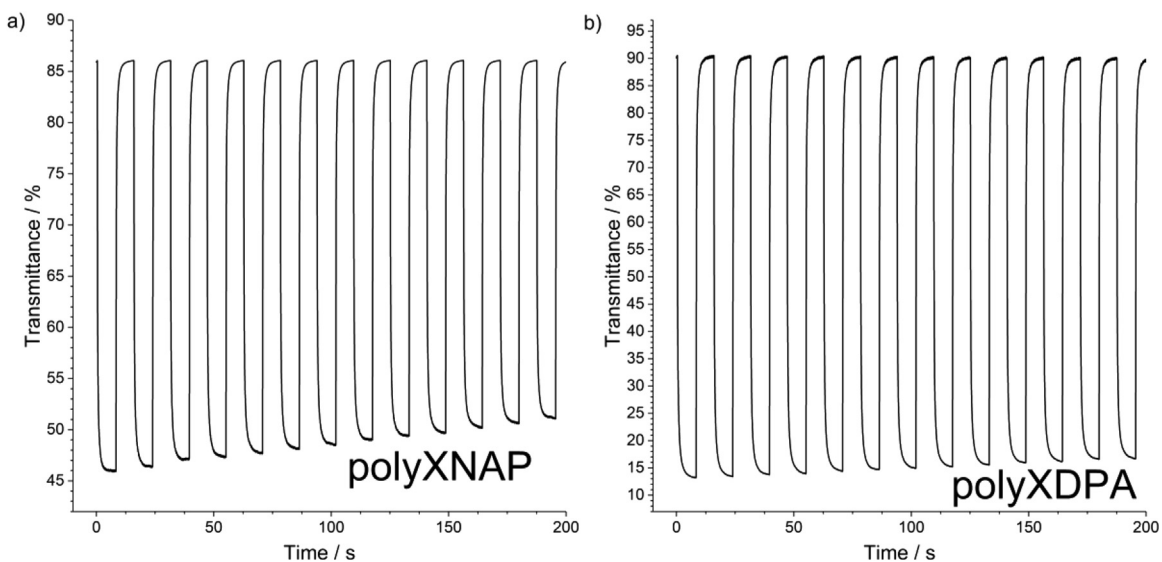
Fig. 4. Electrochromic switching response for polymers on ITO by potentiostatic pulses at −1.0 and 1.0 with 15.6 s period. Transmittances were measured at the absorption peak maxima of the doped polymer film (Table 2).

Table 2
Electrochromic characteristics.

	$T_b[\%]$[a]	$T_c[\%]$[b]	$\lambda_{max}[nm]$[c]	$ORT_{dop}[s]$[d]	$ORT_{dedop}[s]$[d]	$\Delta OD[-]$[e]	$Q_d[mC/cm^2]$[f]	$CE[cm^2/C]$[g]	$CR[-]$[h]
polyXNAP	86.06	45.99	775	1.24	1.20	0.27	3.78	71.98	1.87
polyXDPA	90.54	13.20	710	1.56	1.22	0.84	2.93	285.37	6.85

[a] Transmittance of oxidised polymer at λ_{max}.
[b] Transmittance of neutral polymer at λ_{max}.
[c] The absorption peak of the neutral polymer film.
[d] Optical response time of doping and dedoping process at 95% of the maximum transmittance difference.
[e] Optical Density $\Delta OD = log[T_b/T_c]$.
[f] Charge density calculated in the chronocoulometric experiment [26,44,54].
[g] CE is the colouration efficiency [26,44,54].
[h] The contrast ratio, $CR = T_b(\lambda_{max})/T_c(\lambda_{max})$, where T_b and T_c are the transmittances in the bleached and colored states at λ_{max} of the longest wavelength absorption peak in the neutral state of the film.

4. Conclusions

The investigated xanthone-triarylamines showed very good electrochemical properties as small molecules. Each compounds ability to electropolymerise on the working electrode surface is dictated by its molecular structure; particularly the design of the triarylamine donor moiety. The two formed electropolymers show differences in polymeric structure monitored by the extent of delocalisation during cyclic voltammetric sweeps and UV−visible spectroelectrochemical measurements. Both of the polymers could be used as electrochromic windows but only one, polyXDPA, showed promising properties, with almost 300 cm²/C colouration efficiency and a contrast ratio of almost 7 in NIR area. Materials with such properties could be used as electro responsive optical filters.

Acknowledgements

Appendix A. Supplementary data

Supplementary data related to this article can be found at https://doi.org/10.1016/j.electacta.2018.04.070.

References

[1] A. Pron, P. Gawrys, M. Zagorska, D. Djurado, R. Demadrille, Electroactive materials for organic electronics: preparation strategies, structural aspects and characterization techniques, Chem. Soc. Rev. 39 (2010) 2577–2632, https://doi.org/10.1039/B907999H.
[2] A.W. Hains, Z. Liang, M.A. Woodhouse, B.A. Gregg, Molecular semiconductors in organic photovoltaic cells, Chem. Rev. 110 (2010) 6689–6735, https://doi.org/10.1021/cr9002984.
[3] C. Xia, X. Fan, J. Locklin, R.C. Advincula, A first synthesis of thiophene dendrimers, Org. Lett. 4 (2002) 2067–2070, https://doi.org/10.1021/ol025943a.
[4] K.R. Idzik, P. Ledwon, R. Beckert, S. Golba, J. Frydel, M. Lapkowski, Electrochemical and spectral properties of meta-linked 1,3,5-tris(aryl)benzenes and 2,4,6-tris(aryl)-1-phenoles, and their polymers, Electrochim. Acta 55 (2010) 7419–7426, https://doi.org/10.1016/j.electacta.2010.07.005.
[5] X.B. Sun, Y.Q. Liu, S.Y. Chen, W.F. Qiu, G. Yu, Y.Q. Ma, T. Qi, H.J. Zhang, X.J. Xu, D.B. Zhu, X-shaped electroactive molecular materials based on oligothiophene architectures: facile synthesis and photophysical and electrochemical properties, Adv. Funct. Mater. 16 (2006) 917–925, https://doi.org/10.1002/adfm.200500463.
[6] J.H. Burroughes, D.D.C. Bradley, A.R. Brown, R.N. Marks, K. Mackay, R.H. Friend, P.L. Burns, A.B. Holmes, Light-emitting diodes based on conjugated polymers, Nature 347 (1990) 539–541, https://doi.org/10.1038/347539a0.
[7] A.C. Grimsdale, K. Leok Chan, R.E. Martin, P.G. Jokisz, A.B. Holmes, Synthesis of light-emitting conjugated polymers for applications in electroluminescent devices, Chem. Rev. 109 (2009) 897–1091, https://doi.org/10.1021/cr000013v.
[8] A. Facchetti, π-conjugated polymers for organic electronics and photovoltaic cell applications, Chem. Mater. 23 (2011) 733–758, https://doi.org/10.1021/cm102419z.
[9] M.S. AlSalhi, J. Alam, L.A. Dass, M. Raja, Recent advances in conjugated polymers for light emitting devices, Int. J. Mol. Sci. 12 (2011) 2036–2054, https://doi.org/10.3390/ijms12032036.
[10] S. Chizu, T. Yoshiaki, Y. Takeshi, K. Makoto, D. Shuji, Recent progress of high performance polymer OLED and OPV materials for organic printed electronics, Sci. Technol. Adv. Mater. 15 (2014) 034203, https://doi.org/10.1088/1468-6996/15/3/034203.
[11] L. Liao, Y. Pang, L. Ding, F.E. Karasz, Blue-emitting soluble poly(m-phenylenevinylene) derivatives, Macromolecules 34 (2001) 7300–7305, https://doi.org/10.1021/ma0108923.
[12] L. Akcelrud, Electroluminescent polymers, Prog. Polym. Sci. 28 (2003) 875–962, https://doi.org/10.1016/S0079-6700(02)00140-5.
[13] M. Häussler, J. Liu, R. Zheng, J.W.Y. Lam, A. Qin, B.Z. Tang, Synthesis, thermal stability, and linear and nonlinear optical properties of hyperbranched polyarylenes containing carbazole and/or fluorene moieties, Macromolecules 40 (2007) 1914–1925, https://doi.org/10.1021/ma062346l.
[14] P. Taranekar, T. Fulghum, D. Patton, R. Ponnapati, G. Clyde, R. Advincula, Investigating carbazole jacketed precursor dendrimers: sonochemical synthesis, characterization, and electrochemical crosslinking properties, J. Am. Chem. Soc. 129 (2007) 12537–12548, https://doi.org/10.1021/ja074007t.
[15] J. Heinze, B.A. Frontana-Uribe, S. Ludwigs, Electrochemistry of conducting polymers—persistent models and new concepts, Chem. Rev. 110 (2010) 4724–4771, https://doi.org/10.1021/cr900226k.
[16] A.F. Diaz, J.A. Logan, Electroactive polyaniline films, J. Electroanal. Chem. 111 (1980) 111–114, https://doi.org/10.1016/S0022-0728(80)80081-7.
[17] G. Tourillon, F. Garnier, New electrochemically generated organic conducting polymers, J. Electroanal. Chem. 135 (1982) 173–178, https://doi.org/10.1016/0022-0728(82)90015-8.
[18] R.J. Waltman, J. Bargon, Electrically conducting polymers: a review of the electropolymerization reaction, of the effects of chemical structure on polymer film properties, and of applications towards technology, Can. J. Chem. 64 (1986) 76–95, https://doi.org/10.1139/v86-015.
[19] R.J. Waltman, A.F. Diaz, J. Bargon, The electrochemical oxidation and polymerization of polycyclic hydrocarbons, J. Electrochem. Soc. 132 (1985) 631–634, https://doi.org/10.1149/1.2113918.
[20] T. Lana-Villarreal, J.M. Campina, N. Guijarro, R. Gomez, Solid-state electropolymerization and doping of triphenylamine as a route for electroactive thin films, Phys. Chem. Chem. Phys. 13 (2011) 4013–4021, https://doi.org/10.1039/C0CP01818J.
[21] Y. Shirota, H. Kageyama, Charge Carrier transporting molecular materials and their applications in devices, Chem. Rev. 107 (2007) 953–1010, https://doi.org/10.1021/cr050143.
[22] P. Data, M. Lapkowski, R. Motyka, J. Suwinski, Electrochemistry and spectroelectrochemistry of a novel selenophene-based monomer, Electrochim. Acta 59 (2012) 567–572, https://doi.org/10.1016/j.electacta.2011.11.021.
[23] C.L. Gaupp, D.M. Welsh, R.D. Rauh, J.R. Reynolds, Composite coloration efficiency measurements of electrochromic polymers based on 3,4-alkylenedioxythiophenes, Chem. Mater. 14 (2002) 3964, https://doi.org/10.1021/cm020433w.
[24] P. Data, R. Motyka, M. Lapkowski, J. Suwinski, A.P. Monkman, Spectroelectrochemical analysis of charge carriers as a way of improving poly(p-phenylene)-based electrochromic windows, J. Phys. Chem. C 119 (2015) 20188–20200, https://doi.org/10.1021/acs.jpcc.5b06846.d.
[25] A.L. Dyer, M.R. Craig, J.E. Babiarz, K. Kiyak, J.R. Reynolds, Orange and red to transmissive electrochromic polymers based on electron-rich dioxythiophenes, Macromolecules 43 (2010) 4460–4467, https://doi.org/10.1021/ma100366y.
[26] P. Data, P. Zassowski, M. Lapkowski, W. Domagala, S. Krompiec, T. Flak, M. Penkala, A. Swist, J. Soloducho, W. Danikiewicz, Electrochemical and spectroelectrochemical comparison of alternated monomers and their copolymers based on carbazole and thiophene derivatives, Electrochim. Acta 122 (2014) 118–129, https://doi.org/10.1016/j.electacta.2013.11.167.
[27] K. Laba, P. Data, P. Zassowski, P. Pander, M. Lapkowski, K. Pluta,

A.P. Monkman, Diquinoline derivatives as materials for potential optoelectronic applications, J. Phys. Chem. C 119 (2015) 13129–13137, https://doi.org/10.1021/jp512941z.

[28] P. Pander, P. Data, R. Turczyn, M. Lapkowski, A. Swist, J. Soloducho, A.P. Monkman, Synthesis and characterization of chalcogenophene-based monomers with pyridine acceptor unit, Electrochim. Acta 210 (2016) 773–782, https://doi.org/10.1016/j.electacta.2016.05.185.

[29] H. Shin, Y. Kim, T. Bhuvana, J. Lee, X. Yang, C. Park, E. Kim, Color combination of conductive polymers for black electrochromis, ACS Appl. Mater. Interfaces 4 (2012) 185–191, https://doi.org/10.1021/am201229k.

[30] P. Data, P. Zassowski, M. Lapkowski, J.V. Grazulevicious, N.A. Kukhta, R.R. Reghu, Electrochromic behaviour of triazine based ambipolar compounds, Electrochim. Acta 192 (2016) 283–295, https://doi.org/10.1016/j.electacta.2016.01.208.

[31] H.-S. Liu, B.-C. Pan, D.-C. Huang, Y.-R. Kung, C.-M. Leu, G.-S. Liou, Highly, transparent to truly black electrochromic devices based on an ambipolar system of polyamides and viologen, NPG Asia Mater. 9 (2017) e388, https://doi.org/10.1038/am.2017.57.

[32] E.T. Seo, R.F. Nelson, J.M. Fritsch, L.S. Marcoux, D.W. Leedy, R.N. Adams, Anodic oxidation pathways of aromatic amines. Electrochemical and electron paramagnetic resonance studies, J. Am. Chem. Soc. 88 (1966) 3498–3503, https://doi.org/10.1021/ja00967a006.

[33] P. Data, P. Pander, P. Zassowski, V. Mimaite, K. Karon, M. Lapkowski, J.V. Grazulevicius, P. Slepski, K. Darowicki, Electrochemically induced synthesis of triphenylamine-based polyhydrazones, Electrochim. Acta 230 (2017) 10–21, https://doi.org/10.1016/j.electacta.2017.01.132.

[34] C.-W. Huang, K. Yuan Chiu, S.-H. Cheng, Novel spectral and electrochemical characteristics of triphenylamine-bound zinc porphyrins and their intramolecular energy and electron transfer, Dalton Trans. 0 (2005) 2417–2422, https://doi.org/10.1039/B503683F.

[35] S. Pluczyk, P. Zassowski, R. Rybakiewicz, R. Wielgosz, M. Zagorska, M. Lapkowski, A. Pron, UV-vis and EPR spectroelectrochemical investigations of triarylamine functionalized arylene bisimides, RSC Adv. 5 (2015) 7401–7412, https://doi.org/10.1039/C4RA12603C.

[36] Y. Song, C.A. Di, X. Yang, S. Li, W. Xu, Y. Liu, L. Yang, Z. Shuai, D. Zhang, D. Zhu, A cyclic triphenylamine dimer for organic field-effect transistors with high performance, J. Am. Chem. Soc. 128 (2006) 15940–15941, https://doi.org/10.1021/ja064726s.

[37] H. Xiao, L. Ding, D. Ruan, B. Li, N. Ding, D. Ma, tert-Butylated spirobifluorene derivative incorporating triphenylamine groups: a deep-blue emitter with high thermal stability and good hole transport ability for organic light emitting diode applications, Dyes Pigments 121 (2015) 7–12, https://doi.org/10.1016/j.dyepig.2015.03.027.

[38] Y.N. Luponosov, A.N. Solodukhin, S.A. Ponomarenko, Branched triphenylamine-based oligomers for organic electronics, Polym. Sci. Ser. C 56 (2014) 104–134, https://doi.org/10.1134/S181123821401007X.

[39] M.Y. Wong, E. Zysman-Colman, Purely organic thermally activated delayed fluorescence materials for organic light-emitting diodes, Adv. Mater. 29 (2017), 1605444, https://doi.org/10.1002/adma.201605444.

[40] M. Inoue, T. Serevicius, H. Nakanotani, K. Yoshida, T. Matsushima, S. Juršenas, C. Adachi, Effect of reverse intersystem crossing rate to suppress efficiency roll-off in organic light-emitting diodes with thermally activated delayed

fluorescence emitters, Chem. Phys. Lett. 644 (2016) 62–67, https://doi.org/10.1016/j.cplett.2015.11.042.

[41] H. Nakanotani, T. Higuchi, T. Furukawa, K. Masui, K. Morimoto, K. Numata, H. Tanaka, Y. Sagara, T. Yasuda, C. Adachi, High-efficiency organic light-emitting diodes with fluorescent emitters, Nat. Commun. 5 (2014) 4016, https://doi.org/10.1038/ncomms5016.

[42] H.-M. Wang, S.-H. Hsiao, Ambipolar, multi-electrochromic polypyromellitimides and polynaphthalimides containing di(tert-butyl)-substituted bis(triarylamine) units, J. Mater. Chem. C 2 (2014) 1553–1564, https://doi.org/10.1039/C3TC32005G.

[43] H.-J. Yen, Novel starburst triarylamine-containing electroactive aramids with highly stable electrochromism in near-infrared and visible light regions, Chem. Mater. 23 (2011) 1874–1882, https://doi.org/10.1021/cm103552k.

[44] P.M.S. Monk, R.J. Mortimer, D.R. Rosseinsky, Electrochromism and Electrochromic Devices, Cambridge University Press, Cambridge, 2007.

[45] M.P. Coleman, M.K. Boyd, S-pixyl analogues as photocleavable protecting groups for nucleosides, J. Org. Chem. 67 (2002) 7641–7648, https://doi.org/10.1021/jo026009w.

[46] A.S. Guram, S.L. Buchwald, Palladium-Catalyzed aromatic aminations with in situ generated aminostannanes, J. Am. Chem. Soc. 116 (1994) 7901–7902, https://doi.org/10.1021/ja00096a059.

[47] F. Paul, J. Patt, J.F. Hartwig, Palladium-catalyzed formation of carbon-nitrogen bonds. Reaction intermediates and catalyst improvements in the hetero cross-coupling of aryl halides and tin amides, J. Am. Chem. Soc. 116 (1994) 5969–5970, https://doi.org/10.1021/ja00092a058.

[48] B.K. Sharma, A.M. Shaikh, R.M. Kamble, Synthesis, photophysical, electrochemical and thermal investigation of Triarylamines based on 9H-Xanthen-9-one: yellow–green fluorescent materials, J. Chem. Sci. 127 (2015) 2063–2071, https://doi.org/10.1007/s12039-015-0973-0.

[49] P. Data, P. Pander, M. Lapkowski, A. Swist, J. Soloducho, R.R. Reghu, J.V. Grazulevicius, Unusual properties of electropolymerized 2,7- and 3,6-carbazole derivatives, Electrochim. Acta 128 (2014) 430–438, https://doi.org/10.1016/j.electacta.2013.12.108.

[50] J.-L. Bredas, Mind the gap!, Mater. Horiz. 1 (2014) 17–19, https://doi.org/10.1039/C3MH00098B.

[51] P. Data, M. Lapkowski, R. Motyka, J. Suwinski, Influence of heteroaryl group on electrochemical and spectroscopic properties of conjugated polymers, Electrochim. Acta 83 (2012) 271–282, https://doi.org/10.1016/j.electacta.2012.08.020.

[52] K. Karon, M. Lapkowski, A. Dabuliene, A. Tomkeviciene, N. Kostiv, J.V. Grazulevicius, Spectroelectrochemical characterization of conducting polymers from star-shaped carbazole-triphenylamine compounds, Electrochim. Acta 154 (2015) 119–127.

[53] Hui Huang, Nanjia Zhou, R.P. Ortiz, Z. Chen, S. Loser, S. Zhang, X. Guo, J. Casado, J.T. López Navarrete, X. Yu, A. Facchetti, T.J. Marks, Alkoxy-Functionalized thienyl-vinylene polymers for field effect transistors and all-polymer solar cells, Adv. Funct. Mater. 24 (2014) 2782–2793.

[54] P. Data, M. Lapkowski, R. Motyka, J. Suwinski, Influence of alkyl chain on electrochemical and spectroscopic properties of polyselenophenes, Electrochim. Acta 87 (2013) 438–449, https://doi.org/10.1016/j.electacta.2012.09.077.